Synthesis, Gene Silencing, and Molecular Modeling Studies of 4′-C-Aminomethyl-2′-O-methyl Modified Small Interfering RNAs

Kiran R. Gore,[†] Ganesh N. Nawale,[†] S. Harikrishna,[†] Vinita G. Chittoor,[†] Sushil Kumar Pandey,[†] Claudia Höbartner,[‡] Swati Patankar,[§] and P. I. Pradeepkumar*,[†]

[†]Department of Chemistry, Indian Institute of Technology Bombay, Mumbai 400076, India
[‡]Research Group Nucleic Acid Chemistry, Max Planck Institute for Biophysical Chemistry, Am Fassberg 11, 37077 Göttingen, Germany
[§]Department of Biosciences and Bioengineering, Indian Institute of Technology Bombay, Powai, Mumbai 400076, India

ⓢ *Supporting Information*

ABSTRACT: The linear syntheses of 4′-C-aminomethyl-2′-O-methyl uridine and cytidine nucleoside phosphoramidites were achieved using glucose as the starting material. The modified RNA building blocks were incorporated into small interfering RNAs (siRNAs) by employing solid phase RNA synthesis. Thermal melting studies showed that the modified siRNA duplexes exhibited slightly lower T_m (~1 °C/modification) compared to the unmodified duplex. Molecular dynamics simulations revealed that the 4′-C-aminomethyl-2′-O-methyl modified nucleotides adopt *South*-type conformation in a siRNA duplex, thereby altering the stacking and hydrogen-bonding interactions. These modified siRNAs were also evaluated for their gene silencing efficiency in HeLa cells using a luciferase-based reporter assay. The results indicate that the modifications are well tolerated in various positions of the passenger strand and at the 3′ end of the guide strand but are less tolerated in the seed region of the guide strand. The modified siRNAs exhibited prolonged stability in human serum compared to unmodified siRNA. This work has implications for the use of 4′-C-aminomethyl-2′-O-methyl modified nucleotides to overcome some of the challenges associated with the therapeutic utilities of siRNAs.
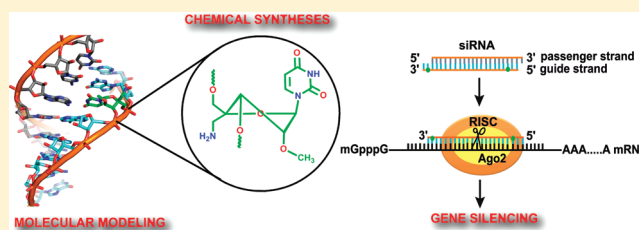
■ INTRODUCTION

RNA interference (RNAi) is a post-transcriptional gene silencing mechanism, triggered by double-stranded RNAs called small interfering RNAs (siRNAs), which are 19−21 base pairs long and contain two nucleotide 3′ overhangs.[1−3] One strand of the siRNA is the passenger strand with the same sequence as the target mRNA, while the other strand is the guide strand, which has the complementary sequence to the target.[4] The RNAi mechanism involves loading of siRNA into the RNA induced silencing complex (RISC), which is the key cellular machinery involved in the RNA-mediated gene silencing process.[4,5] Mammalian RISC contains an endonuclease enzyme, Argonaute 2 (Ago2), which is responsible for the removal of the passenger strand and the guide-strand-mediated site-specific cleavage of mRNA.[4,5]

Because RNAi is a powerful tool, which can be used to silence expression of any particular gene, it has created great opportunities to harness the therapeutic potentials of siRNAs. Several siRNA-based molecules are currently being evaluated in the clinic.[6,7] Despite their significant potential benefits, numerous challenges are associated with the therapeutic applications of siRNAs.[8] These include their susceptibility toward nucleases,[9] off-target effects,[10,11] innate immune stimulation,[12] and inefficient *in vivo* delivery.[13] These challenges can be addressed to a large extent by the rational incorporation

of chemical modifications in the siRNAs.[8,14−16] Various types of chemical modifications in the sugar [2′-O-methyl,[17] 2′-fluoro,[18] locked nucleic acid (LNA)[19] and its analogues,[20,21] 2′-methoxyethyl (MOE),[17] 2′-fluoroarabino (FANA),[22] 2′-azido[23] etc.], phosphate backbone [phosphorothioate (PS),[24] boranophosphate[25] etc.], and nucleobase (5-methyl,[26] 5-propargyl,[26] 8-oxoguanosine,[27] N^2-cyclopentylguanosine,[28] etc.) have been used in siRNAs. Many of these modifications show compatibility to RNAi machinery depending on their numbers and positions in a siRNA duplex. However, studies have shown that each modification has its advantages and drawbacks.[8]

Because Ago2 enzyme is highly sensitive to changes in the grooves and the RNA backbone, many of the currently available modifications are not suitable for extensive modification of siRNA duplexes.[8,29] Therefore, modifications, which can be used in minimal number and can impart high therapeutic potency, are of great value. Toward this end "dual modifications", which harbor two modified functionalities on a single ribose skeleton such as 2′-O-methyl-4′-thioRNA (Me-SRNA),[30] 2′-fluoro-4′-thioRNA (F-SRNA),[30] and 4′-thio-2′-fluoro-β-D-arabinonucleic acid (S-FANA)[31] units, have been

incorporated into siRNAs. The Me-SRNA showed remarkable increase in nuclease stability compared to the 2′-O-methyl and 2′-F modified RNAs.[30] F-SRNA showed moderate improvement in target binding affinity compared to Me-SRNA. S-FANA modification has shown compatibility with the RNAi machinery.[31] These interesting findings provide opportunities to explore new "dual modifications" in siRNAs.

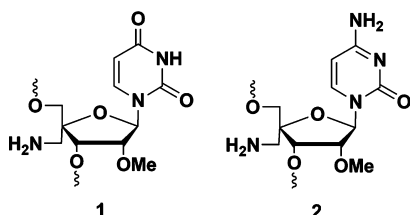Here we report the synthesis of 4′-C-aminomethyl-2′-O-methyl uridine and cytidine (Figure 1) modified siRNAs.

Figure 1. Structures of 4′-C-aminomethyl-2′-O-methyl uridine (**1**) and cytidine (**2**) siRNA modifications reported in this study.

Though 4′-C-aminomethyl-2′-O-methyl thymidine modified DNAs have been reported by Wengel and co-workers,[32,33] the synthesis of the corresponding uridine and cytidine units or their use in siRNAs has not been found in the literature. We hypothesize that this modification could impart many desired therapeutic properties to siRNA. The 4′-C-aminomethyl-2′-O-methyl modification, being anchored in the sugar, is expected to be positioned in the minor groove of a siRNA/mRNA duplex. This is advantageous since the minor groove modifications such as 2′-O-methyl and 2′-fluoro are known to inhibit immune stimulation of siRNAs.[34] Also, the 2′-O-methyl group is expected to tune the sugar conformation to C3′-endo, which is in fact necessary for forming the desired A-type RNA/RNA helix and also to enhance the target mRNA binding affinity.[35] The 2′-O-methyl group at position 2 in the seed region of the guide strand has been shown to reduce off-target effects significantly.[10,11] The aliphatic primary amine at the 4′-position can get protonated under physiological pH. This will reduce the net negative charge of the RNA and thereby enhance its cellular uptake.[36] Moreover, the positively charged amino group could enhance the nuclease stability of siRNAs.[37,38] In this work, we examine the effect of the 4′-C-aminomethyl-2′-O-methyl modification on thermal stability, serum stability, and RNAi activity. In addition, MD stimulations were carried out to decipher the structural and dynamic features of this modification in siRNA duplexes.

Scheme 1. Synthesis of 4′-C-Aminomethyl-2′-O-methyl Uridine Phosphoramidite[a]
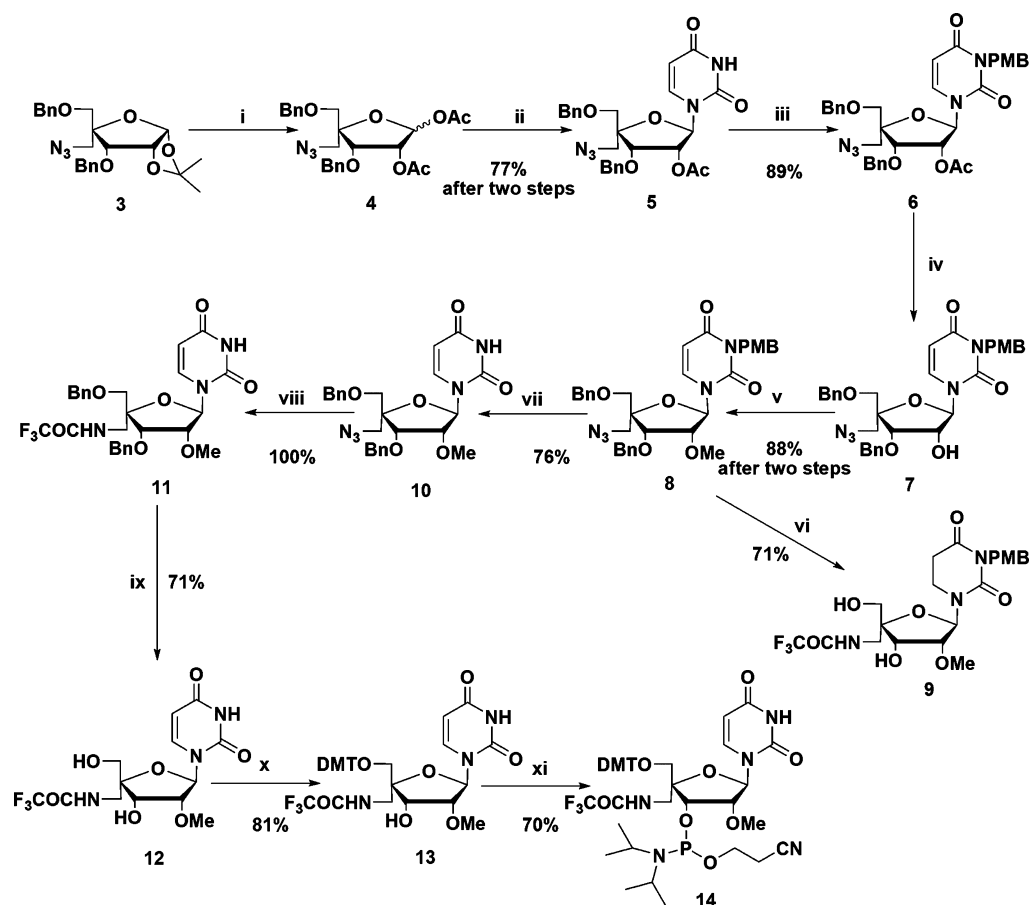
[a]Reagents and conditions: (i) acetic acid, triflic acid, acetic anhydride, rt, 3 h; (ii) uracil, N,O-bis(trimethylsilyl) acetamide, TMSOTf, CH₃CN, 80 °C, overnight; (iii) 4-methoxy benzyl chloride, DBU, CH₃CN, rt, 6 h; (iv) NaOMe, MeOH, rt, 3 h; (v) NaH, MeI, THF, rt, 3 h; (vi) (a) Pd(OH)₂, ammonium formate, MeOH, reflux, 6 h, (b) CF₃COOEt, Et₃N, MeOH, rt, overnight; (vii) CAN, CH₃CN/H₂O (9:1), rt, 55 h; (viii) (a) PPh₃, THF, H₂O, 45 °C, 4 h, (b) CF₃COOEt, Et₃N, rt, overnight; (ix) 10% Pd/C, EtOH, 70 °C, 16 h; (x) DMT-Cl, pyridine, rt, 24 h; (xi) NC(CH₂)₂OP(Cl)N(iPr)₂, DIPEA, DCM, rt, 75 min.

Scheme 2. Synthesis of 4′-C-Aminomethyl-2′-O-methyl Cytidine Phosphoramidite[a]
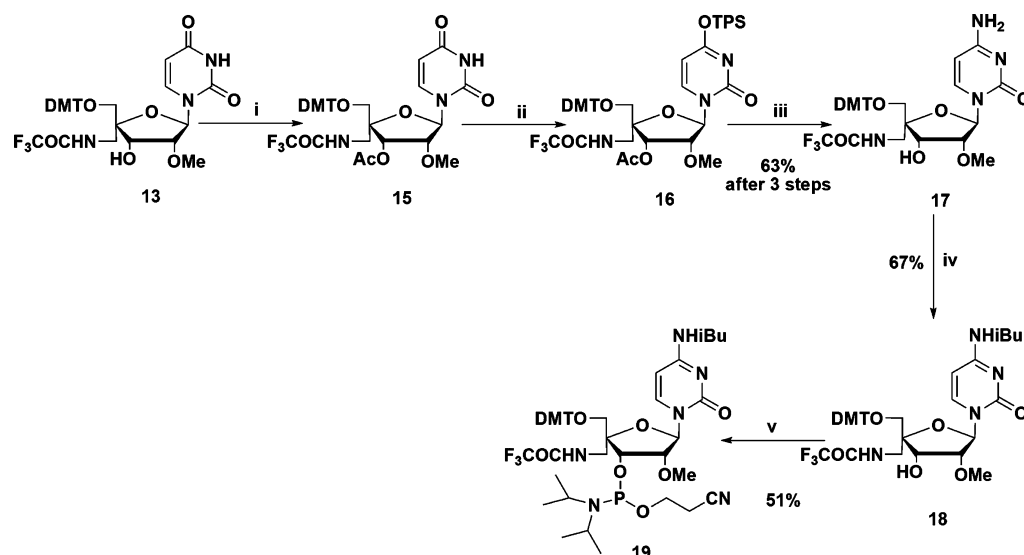
[a]Reagents and conditions: (i) acetic anhydride, pyridine, rt, overnight; (ii) TPS-Cl, DMAP, Et$_3$N, DCM, rt, 5 h; (iii) 30% aq NH$_3$, THF, rt, overnight; (iv) (a) TMS-Cl, pyridine, rt, 1 h, (b) iBu-Cl, rt, 3 h; (v) CN(CH$_2$)$_2$OP(Cl)N(iPr)$_2$, DIPEA, DCM, rt, 40 min.

Table 1. Sequences of siRNA Duplexes Reported in This Study and Representative T_m Values

Name	Sequence of passenger (5'-3', above) and guide strand (3'-5', below)	T_m[a]	ΔT_m[b]/mod.
3R-2R	GGCCUUUCACUACUCCUACTT TTCCGGAAAGUGAUGAGGAUGA	79.0 ± 0.1	
9R-2R	GGCCUUUCACUACUCCUACTT TTCCGGAAAGUGAUGAGGAUGA	78.4 ± 0.2	−0.6
12R-2R	GGCCUUUCACUACUCCUACUT TTCCGGAAAGUGAUGAGGAUGA	76.5 ± 0.3	−1.3
3R-22R	GGCCUUUCACUACUCCUACTT TTCCGGAAAGUGAUGAGGAUGA	78.3 ± 0.2	−0.7
3R-7R	GGCCUUUCACUACUCCUACTT TUCCGGAAAGUGAUGAGGAUGA	77.2 ± 0.3	−0.9
16R-2R	GGCCUUUCACUACUCCUACTT TUCCGGAAAGUGAUGAGGAUGA	78.5 ± 0.2	−0.5
6R-2R	GGCCUUUCACUACUCCUACTT TTCCGGAAAGUGAUGAGGAUGA	n.d.[c]	
6R-7R	GGCCUUUCACUACUCCUACTT TUCCGGAAAGUGAUGAGGAUGA	n.d.	
3R-29R	GGCCUUUCACUACUCCUACTT TUCCGGAAAGUGAUGAGGAUGA	80.0 ± 0.1	+0.5
Scrambled (SC)	UAAGGCUAUGAAGAGAUACTT TTAUUCCGAUACUUCUCUAUGA	n.d.	

[a]T_m represents melting temperatures for unmodified, 4′-C-aminomethyl-2′-O-methyl (green) and 2′-O-methyl (red) modified siRNA duplexes.
[b]ΔT_m represents [T_m (RNAmod) − T_m (RNAunmod)]. The T_m values were determined using 1 μM siRNA in T_m buffer (100 mM NaCl, 10 mM Na$_2$PO$_4$, 0.1 mM EDTA, pH 7.4). All experiments were triplicated, and the T_m values reported are the average of 3 measurements with the estimated standard deviation. [c]n.d. = not determined

■ RESULTS AND DISCUSSION

Synthesis of 4′-C-Aminomethyl-2′-O-methyl Modified Uridine and Cytidine Phosphoramidites and Modified RNAs. The synthesis of 4′-C-aminomethyl-2′-O-methyl modified uridine and cytidine blocks started from the known azido sugar precursor **3** as shown in Scheme 1. The azido sugar **3** was prepared from D-glucose using reported procedures.[39,40,33] Compound **3** was converted to diacetate **4** using a mixture of acetic acid, acetic anhydride, and triflic acid by stirring at room

temperature for 3 h. Without further purification, using a modified Vorbruggen reaction,[41] the diacetate **4** was subjected to base coupling using silylated uracil (N,O-bis(trimethylsilyl)acetamide and uracil) and trimethylsilyl triflate in acetonitrile at 80 °C for overnight to furnish nucleoside **5** in 77% yield. The β-configuration of the uracil base in **5** was confirmed by 1D NOE. The H2′ of the sugar showed 8% NOE enhancement when H6 of the base was irradiated. The N^3 of nucleoside **5** was protected with 4-methoxy benzyl chloride (PMB-Cl) using 1,8-

diazabicyclo[5.4.0]undec-7-ene (DBU) as a base in acetonitrile at room temperature for 6 h to furnish compound **6** in 89% yield.[42] The 2′-acetate group of nucleoside **6** was hydrolyzed using 1 M sodium methoxide in methanol at room temperature for 3 h to yield 2′-hydroxy nucleoside **7**. Crude **7** was directly methylated by using methyl iodide (MeI) and sodium hydride (NaH) in tetrahydrofuran (THF) at room temperature for 3 h to obtain 2′-*O*-methyl nucleoside **8** in 88% yield.[41] The debenzylation and azide reduction of **8** were attempted using ammonium formate and 20% Pd(OH)$_2$ in methanol at reflux condition for 6 h, followed by protection of the 4′-CH$_2$NH$_2$ group using ethyl trifluoro acetate (CF$_3$COOEt) and triethyl-amine (Et$_3$N) in MeOH at room temperature overnight.[41,43] However, during these processes, the C5−C6 double bond of the uridine of **8** was reduced to yield dihydrouridine nucleoside **9** bearing a PMB group in 71% yield. Similar to our observation, the formation of undesired dihydrouridine product has been reported during the debenzylation of LNA building blocks using 20% Pd(OH)$_2$.[44] To solve this problem, we employed an alternative strategy for deprotection involving multiple steps. First, the deprotection of the PMB group of compound **8** was performed using ceric ammonium nitrate (CAN) in aqueous acetonitrile (9:1) at room temperature for 55 h to furnish compound **10** in 76% yield.[43] Reduction of the azide group of compound **10** was carried out with triphenylphosphine (PPh$_3$) in THF at 45 °C for 4 h to furnish the crude amine, which was subsequently protected by using CF$_3$COOEt at room temperature for overnight to afford the protected nucleoside **11** in quantitative yield.[45] Debenzylation of compound **11** was carried out with 10% Pd/C in EtOH at 70 °C for 16 h to give the deprotected nucleoside **12** in 71% yield. The 5′-OH of nucleoside **12** was protected using 4,4′-dimethoxytrityl chloride (DMT-Cl) in pyridine at room temperature for 24 h to furnish compound **13** in 81% yield.[43] Nucleoside **13** was phosphitylated using *2-cyanoethyl- N,N*-diisopropylchloro phosphoramidite (CEP-Cl) and *N,N*-diiso-propylethylamine (DIPEA) in dichloromethane (DCM) at room temperature for 75 min to furnish the phosphoramidite **14** in 70% yield.[46]

The synthesis of cytidine phosphoramidite **19** was started from compound **13** as outlined in Scheme 2. Acetylation of DMT uridine nucleoside **13** was achieved using acetic anhydride in pyridine to afford acetylated nucleoside **15**. The crude **15** was converted to 2,4,6-triisopropylbenzenesulphonyl (TPS) derivative **16** using TPS-Cl, 4-dimethylaminopyridine (DMAP), and Et$_3$N in DCM at room temperature. Without further purification, the TPS derivative **16** was treated with 30% aqueous NH$_3$ in THF for 12 h at room temperature to furnish cytidine nucleoside **17** in 63% yield (after three steps).[47] The exocyclic amino group of **17** was protected using isobutyryl chloride (*i*Bu-Cl) in pyridine at room temperature for 3 h employing transient protection of the hydroxyl group by trimethylsilyl (TMS-Cl) to furnish compound **18** in 67% yield.[43] The cytidine nucleoside **18** was phosphitylated using CEP-Cl and DIPEA in DCM at room temperature for 40 min to furnish the phosphoramidite **19** in 51% yield.

The modified phosphoramidites **14** and **19** were successfully incorporated into siRNAs (Table 1), designed to target the *Renilla* luciferase gene using standard solid phase RNA synthesis. The chemical modifications are judiciously incorporated at various positions in the passenger strand and guide strands. The RNAs were deprotected using standard conditions[48,49] and purified by 20% denaturing PAGE. The

integrity of the RNAs was confirmed by negative mode ESI-MS analysis (Table S10, Supporting Information).

Thermal Melting Studies of siRNA Duplexes. To explore the effect of chemical modification on siRNA duplex stability, UV-melting studies were performed in phosphate buffer (pH 7.4) containing 100 mM NaCl (Figure S1, Supporting Information). The T_m values are reported in Table 1. Incorporation of 2′-*O*-methyl modification in an siRNA duplex enhanced the T_m by 0.5 °C/modification, which is in agreement with the previous studies.[50] In contrast, depending upon the position in the siRNA, the presence of a single 4′-*C*-aminomethyl-2′-*O*-methyl uridine/cytidine or two uridines decreased the T_m by 0.5−1.3 °C/modification. A similar decrease in T_m (∼2.6 °C/modification) was observed when 4′-*C*-aminomethyl-2′-*O*-methyl thymidine modifications were incorporated into a 2′-*O*-methyl RNA.[33] Matsuda and co-workers also showed that various 4′-*C*-aminoalkyl deoxythymi-dines cause a slight decrease in melting temperatures of DNA-RNA duplexes (∼1 °C per modification).[38] The lower T_m values indicate that the presence of the 4′-*C*-aminomethyl group may have affected the sugar conformation and the hydration at the minor groove, thereby creating disturbances in the stacking and hydrogen bonding interactions. We have addressed these aspects in detail in the molecular modeling section. It should be noted that the slight decrease in thermal stability observed for 4′-*C*-aminomethyl-2′-*O*-methyl uridine and cytidine modified siRNAs was not detrimental for RNAi activity (see the following section for details).

RNA Interference Studies in Cellular Systems. The modified siRNAs were tested for their RNAi efficiency using transfection studies of a luciferase reporter system in HeLa cells. Since the modified siRNAs targeted the *Renilla* luciferase gene, the psiCHECK2 plasmid containing *Renilla* (target) and *Firefly* (control) luciferase genes was used as the reporter system. Lipofectamine-2000 was used as transfection agent for the plasmid and siRNA delivery.[22] The HeLa cells were transfected with siRNA (33 nM), and expression of both luciferase genes was analyzed after 48 h using the dual luciferase reporter assay (DLRA). The scrambled (SC) siRNA was used as negative control in the experiments. Only psiCHECK2 plasmid was used in the positive control (PC) experiments. Gene silencing efficiency was measured by dividing *Renilla* luciferase light units by *Firefly* luciferase light units and normalized with respect to the positive control. Efficient gene silencing is indicated by low normalized ratios of *Renilla*/*Firefly* luciferase activity. The results are summarized in Figure 2.

The results showed that the modifications are well tolerated at various positions in the passenger strand of siRNA. All passenger strand modified siRNA duplexes such as **6R-2R**, **9R-2R**, and **16R-2R** showed almost no loss of RNAi activity when compared to the unmodified duplex, **3R-2R**. The modification in the 3′-overhang of passenger strand as in **12R-2R** was also well tolerated. Therefore, it is clear that the passenger strand modifications do not disturb the binding or function of Ago2 protein in the RISC. The effect of modifications in the guide strand was found to be position-dependent. The cytidine modification toward the 3′-end of the guide strand as seen in **3R-22R** is well tolerated. The modification at position 3 of the seed region of the guide strand as in **3R-7R** and **6R-7R** showed decrease in RNAi activity by 35% and 45% respectively. It should be noted that the 2′-*O*-methyl modified siRNA duplex, **3R-29R**, in which similar positions are modified as **3R-7R**, retained the RNAi activity. This shows that the decrease in
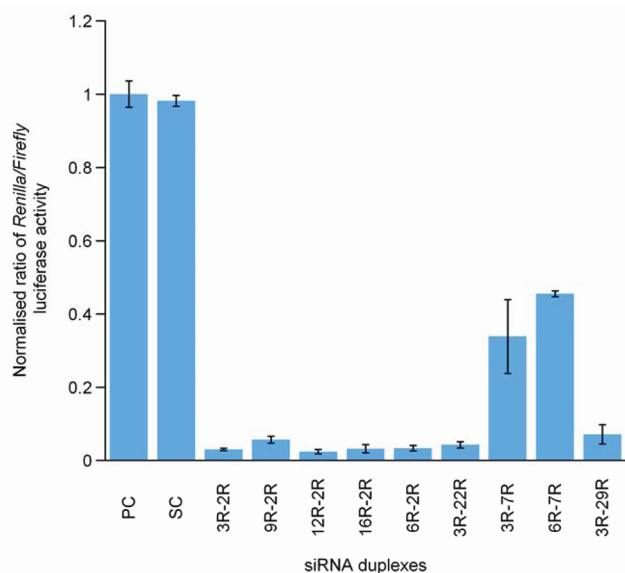
Figure 2. RNAi activity of unmodified and modified siRNAs after 48 h of transfection. HeLa cells were transfected with psiCHECK2 plasmid and siRNAs. Normalized luciferase activity was measured by dividing *Renilla* luciferase light units by *Firefly* luciferase light units and normalized with respect to the positive control (PC, no siRNA). SC denotes scrambled siRNA. Statistical analyses between individual groups were performed by a Student *t* test; a *P* value of <0.05 was considered statistically significant. All error bars represent standard error of the mean (SEM) with $n = 4$.

RNAi activity of the seed region modified duplexes is due to the presence of the 4′-*C*-aminomethyl group, which perhaps hinders a key nucleic acid−protein interaction of the RNAi machinery. This would be expected as the seed region is very important in recognizing the target mRNA sequence.[10] This position has also been shown to play an important role in the formation of the RISC complex, since the MID domain of Ago2 strongly interacts with the 5′-end of the guide strand.[8,51]

Serum Stability Studies. Unmodified siRNAs are highly unstable in serum because of their susceptibility to rapid degradation by nuclease enzymes. Therefore, chemical modifications can increase the half-life of siRNAs and thereby prolong RNAi activity *in vivo*.[8] We assessed the effect of chemical modifications on the stability in human serum of two modified siRNA duplexes: **3R-22R**, which shows *in vivo* RNAi activity similar to that of the unmodified duplex **3R-2R**, and **3R-7R**, which shows reduced *in vivo* RNAi activity compared to that of **3R-2R**. Serum stability of these modified siRNAs was compared with that of the unmodified siRNA. The ^{32}P-labeled modified guide strands **2R**, **22R**, and **7R** were annealed with cold complementary unmodified passenger strand **3R**, and incubated in 10% human serum. Their stability toward serum derived nuclease digestion at various incubation time points was analyzed by denaturing PAGE (Figure 3). The unmodified siRNA duplex was 100% degraded by serum nucleases within 1 h of incubation time. The modified siRNA duplexes were found to be stable for an extended period of time compared to the unmodified siRNA.

The **3R-22R** siRNA with just one cytidine modification toward the 3′-end of the guide strand was intact for 2 h in serum. The **3R-7R** having modifications in position 3 of the seed region and in the overhang was found to be intact up to 8 h. These results clearly show that overhang modifications
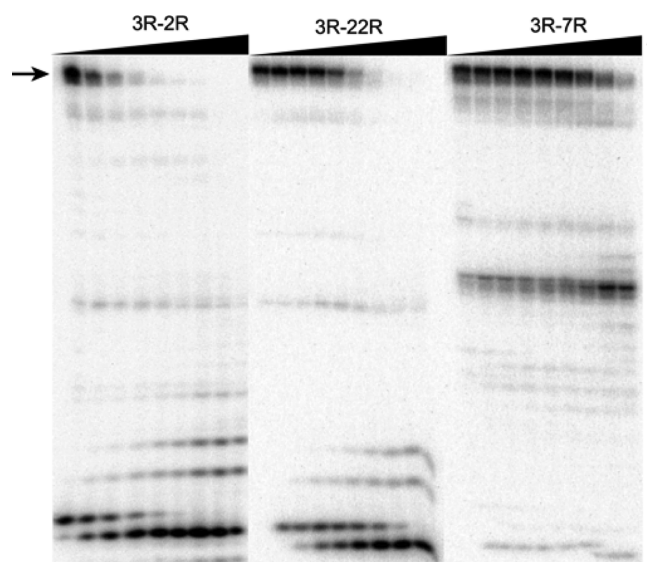

Figure 3. PAGE denoting stability of siRNA duplexes (1.5 μM) in human serum. ^{32}P-labeled siRNA guide strands **2R**, **22R**, and **7R** annealed with cold complementary passenger strand **3R** and incubated in 10% human serum for various time points (*t* = 0, 0.25, 0.5, 1, 2, 4, 8, 22, and 44 h). The intensity of the full-length siRNA bands decreases with increase in incubation time. The arrow represents the full length siRNA guide strand.

increase the serum stability considerably. However, we expected a higher enhancement of the serum stability, since protonated 2′- and 4′-aminoalkyl groups were reported to generate unfavorable electrostatic interactions with the cationic domain of nuclease enzymes.[38,52] The MD simulation studies (see the following section for details) have shown that the 4′-*C*-aminomethyl group in the sugar is flexible and does move away from phosphate group without having any significant electrostatic interaction. This may be the reason for the moderate serum stability observed for the modified siRNAs. Keeping in view the tolerance of 4′-*C*-aminomethyl-2′-*O*-methyl modifications at the 3′-ends of siRNA by the RNAi machinery, our results indicate that introduction of 1−2 modifications at the 3′-ends will be a reliable strategy to enhance serum stability.

Molecular Modeling Studies. The goal of this MD simulation study was to explore the real time dynamics of the solvated siRNA duplexes and to elucidate atomic-resolution details of the structure. Also, the effect of 4′-*C*-aminomethyl-2′-*O*-methyl modified nucleotides on the thermal stability and nuclease stability of siRNA duplexes could be addressed using MD simulation. The two modified siRNA duplexes **3R-7R** and **6R-7R** were chosen for MD studies (Table 1). The siRNA duplex **3R-7R** contains modified uridine at positions 3 and 21 of the guide strand. Here, the modifications lie in the seed region and the 3′ overhang of siRNA duplex. The siRNA duplex **6R-7R** contains four modifications, two at the 5′ end of the passenger strand, one at the seed region, and the other at the 3′ overhang of the guide strand. The unmodified siRNA duplex **3R-2R** was used to compare the structural variability in the modified duplex after 20 ns of MD simulation.

The geometry of 4′-*C*-aminomethyl-2′-*O*-methyl nucleotide was optimized (HF/6-31G*), using Gaussian03,[53] which showed the C3′-endo sugar conformer (Figure S2, Supporting Information). Using the antechamber RESP fitting procedure, the charges for the modified uridine atoms were obtained. The new force field parameters and RESP charges derived for

modified nucleotides were incorporated into the siRNA duplex at respective positions and solvated using water. The solvated siRNA system was then subjected to equilibration, followed by unrestrained MD simulation for 20 ns using AMBER 10.[54] All three duplexes were started with A-form RNA geometry and retained this general form over 20 ns of MD simulation (Figure S3, Supporting Information).

The stability of RNA duplex was monitored by calculating the root-mean-square deviation (rmsd, only heavy atoms) of the conformation evolved during each picosecond of MD simulation (Figure S4, Supporting Information). The rmsd graph over 20 ns trajectory showed that modified duplexes form more flexible structures when compared to the unmodified siRNA duplex. All three duplexes were stabilized and the rmsd converged after 4−5 ns. The positional rmsd calculations around the modified positions (Table S1, Supporting Information) suggest that the modified nucleotides in the helical region of the passenger and the guide strand and also at the overhang region of guide strand are highly flexible. The root-mean-square fluctuation (rmsf) of backbone atoms was also calculated for each duplex (Figure S5, Supporting Information). The rmsf values imply that RNA backbones of modified duplexes were more flexible (rmsf = 7.0 Å) than the unmodified siRNA duplex (rmsf = 5.2 Å).

In order to probe the influence of 4′-C-aminomethyl-2′-O-methyl modification on the sugar puckering, the percentage of C3′-endo sugar conformation was calculated from 20 ns MD trajectories (Figure S6, Supporting Information). Previous studies have shown that natural 2′-OH, and 2′-O-methyl modification in the ribose sugar drives the sugar conformation strongly to *North*-type C3′-endo pucker in an RNA duplex.[55−57] This behavior was also expected for the 4′-C-aminomethyl-2′-O-methyl modified nucleotides. In contrast, strong *South*-type C2′-endo conformation was significantly visible at the modified nucleotide positions of **3R-7R** and **6R-7R** (Figure 4 and Figure
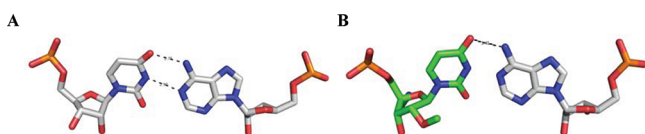

Figure 4. MD snapshots at the modified positions showing the base pairing nucleotide (U-A) and the nature of sugar conformation. (A) Nucleotides of the unmodified siRNA in C3′-endo sugar conformation. (B) 4′-C-Aminomethyl-2′-O-methyl (green) nucleotide of the modified siRNA in C2′-endo sugar conformation. Black dotted lines represent the hydrogen bond interaction between the bases.

S6, Supporting Information). The amplitude of the pseudo rotational angle (*tm*),[58] which represents the nature of four dihedral angles in sugar, showed that all of the unmodified nucleotides in the modified siRNA duplexes retained the native C3′-endo sugar conformation (Figure S6, Supporting Information). The presence of C2′-endo puckered sugars in a predominately C3′-endo dominated A-type helix is likely to be responsible for the slight loss in the thermodynamic stability (∼1 °C/modification) observed for the modified siRNA duplexes. It is reported in the literature that some of the 2′-modifications such as 2′-amino[59] and 2′-amido[60] decrease the thermodynamic stability of RNA/RNA duplex by around 4.3 and 7.3 °C per modification, respectively. Also, the presence of a single 2′-S-methyl,[61,62] and 2′-alkyl[63] modification in a DNA/RNA duplex decreases the thermodynamic stability by around

1.5 and 1.7 °C, respectively. NMR studies at the nucleoside level, DFT calculations performed in both gas phase and in solution for 2′-amino substituted residues,[59,60,64] and MD simulations for the 2′-S-methyl modified duplex[65] all suggest that the S type C2′-endo puckering is energetically favored by these modifications. These studies identified that a combination of steric factors, reduced electronegativity, weaker gauche effect, and reduced hydration are responsible for the adaptation of C2′-endo conformation, which causes the duplex destabilization. In contrast, X-ray structural data of 2′-amino,[66] 2′-amido,[66] and 2′-S-methyl[67] modified duplexes reveal that modified nucleotides switch to C3′-endo conformation in the crystal state. It is interesting to note that recent Selective 2′-Hydroxyl acylation Analyzed by Primer Extension (SHAPE) experiments underscore the fact that local conformational changes of the sugar moieties in an RNA duplex can be induced by the buffer conditions used for crystallization.[66,68] Therefore, the conformational flexibility and the sugar pucker preference of modified nucleotides responsible for changes in the thermodynamic stability of RNA duplexes may not be evident from the crystal structures.

The conformation of phosphodiester backbone angles ($\alpha-\zeta$), which are closely related to sugar puckering, was found to be *gauche⁻ trans* (g^- t) in the 4′-C-aminomethyl-2′-O-methyl modified positions of the siRNA duplex. The γ angle (C4′−C5′) fluctuated because of the flexible movement of 4′-C-aminomethyl modification. As a result, the expected electrostatic interaction between phosphate group and the aminomethyl group was not observed. The alternative sugar and phosphate conformations in RNA duplex are known to increase the minor groove widths,[69] and this was in fact observed in the modified siRNA duplexes (Figure S8, Supporting Information). To characterize the general structure and dynamic features of the duplexes, we calculated the interstrand and intrastrand phosphate distances. The interstrand phosphate distances of unmodified and modified duplexes depict that all duplexes are in its secure girth (Figure S8, Supporting Information). At the modified nucleotide position, the interstrand phosphate distance was elongated up to 23 Å. The nucleotides in the unmodified siRNA duplex have interstrand phosphate distances of only 18 Å. Also, the intrastrand phosphate distances of modified nucleotides extend up to 7.0 Å compared to the 5.9 Å distances of unmodified nucleotides in siRNA (Figures S9−S11, Supporting Information). This longer distance means that the 4′-C-aminomethyl-2′-O-methyl modified nucleotides deviate from the typical layout of A-form helix, thereby affecting the groove geometry.

Since aqueous solvent performs a major role in the nucleic acid structure stability and dynamics,[70] the first hydration shell (<3.0 Å) of the duplex groove and phosphate backbone were computed (Table S2, Supporting Information). The higher thermodynamic stability of RNA over DNA is often ascribed to the presence of a 2′-OH group, which can form a stable solute−solvent interaction and contribute to the stabilization of the hydration shell.[71] RNA duplexes containing 2′-O-methyl modified nucleotides are more stable than the unmodified nucleotides because of long-lived hydration patterns observed in their rigid grooves.[72] Our MD simulation studies of modified siRNA duplexes showed that 4′-C-aminomethyl-2′-O-methylated nucleotides failed to create optimal water binding pockets, which could unfavorably contribute to the thermodynamics of hydration. Minor groove hydration in the unmodified siRNA was found to be higher (∼17 water molecules) than in the

modified siRNA duplexes (~10 water molecules) (Table S2, Supporting Information). The flexibility of helices and long inter- and intrastrand phosphate distances led to unstable minor groove dimensions in the modified siRNA duplex and thus failed to hold the water molecule compactly (Figure S12, Supporting Information). The hydration numbers for backbone atoms and major grooves were also calculated, which revealed that backbone atoms and major grooves in the modified and unmodified duplexes were almost equally hydrated.

The helical deformation and stacking parameters were calculated for all of the duplexes to delineate the effects of modification on helical and stacking stability of RNA. The overall results of these parameters indicate that the modification affects the stacking and helical stability of siRNA (Figure 5). The values of buckle, open angle, stagger, propeller,
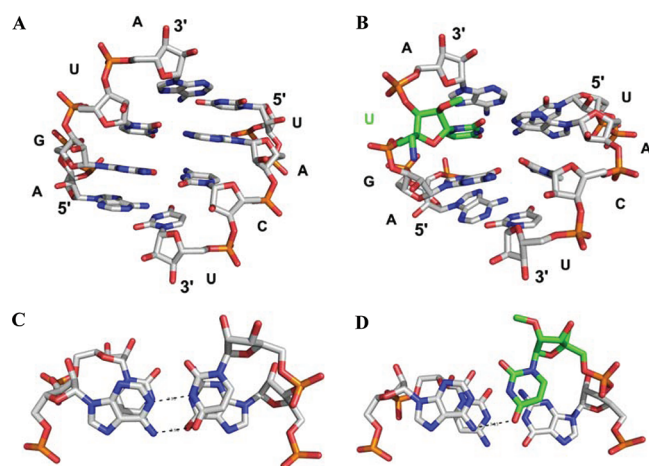

Figure 5. Final MD snapshot of the duplexes at the unmodified and modified region (helical and top view) captured after 20 ns. (A) Unmodified siRNA duplex, **3R-2R** shows well stacked architecture of nucleotides. (B) 4′-*C*-Aminomethyl-2′-*O*-methyl modification (green) in siRNA duplex, **3R-7R,** shows disturbance in stacking interaction in the helical region. (C) Hydrogen bonding and stacking interaction between the two successive nucleotide pairs (A-U, C-G) of unmodified siRNA duplex, **3R-2R.** (D) Disturbed stacking and hydrogen bond interactions at the modified nucleotide (green) of siRNA duplex, **3R-7R.** Black dotted lines in panels C and D represent the hydrogen bond interaction between the bases.

and rise at the unmodified regions of the helices in **3R-7R** and in the unmodified siRNA **3R-2R** were found to be similar (Table S3 and S4, Supporting Information). On the other hand, siRNA duplex **6R-7R** showed higher values (up to 30 Å) of buckle and open angle parameters at modified nucleotide positions (Table S5, Supporting Information). Moreover, stretch and shear parameters were found to be higher for the modified siRNAs than in the unmodified duplex (Tables S4 and S5, Supporting Information). These observations indicate that the minor and major groove widths were fluctuating during simulation. Of the six intrastrand stacking parameters, there was less deviation in roll and rise parameters of modified siRNA in comparison to the unmodified siRNA. However, in the modified duplexes, twist and tilt angles were highly deviated (Table S6 and S7, Supporting Information); this reflects slight unwinding of the helix.[73]

Frequency of chi (χ) angle at the junction of sugar and base was determined for modified nucleotides in **3R-7R** and **6R-7R** and compared with the unmodified nucleotides at respective

position in **3R-2R** (Figure S13, Supporting Information). The capability of holding the base in proper orientation, such that it can form stable hydrogen bond and stacking interaction with nearby and pairing base, can be explained by the χ angle.[74] The χ angle for typical A-type RNA is −160° and for DNA is −120°.[75] Here, for the 4′-*C*-aminomethyl-2′-*O*-methyl modified nucleotides the χ angle was found to be −120° (Figure S13, Supporting Information). This shows that 4′-*C*-aminomethyl-2′-*O*-methyl modified nucleotides deviate from the original RNA type to DNA type, which reflects a scuffle in hydrogen bond and stacking interactions. To address this in detail, the occupancy of two hydrogen bonds between the modified nucleotide and the pairing base was determined. The hydrogen bond occupancy was lacking up to 50% at the modified regions (Figure 5 and Table S8, Supporting Information), which was obviously due to the flexibility of backbone atoms and deviated χ angle.

To obtain deeper insights into the energetics of the hydrogen bond and stacking interactions at the modified nucleotides in the siRNA, the single point energy at DFT (MP2(full)/6-311G*) level was computed (Table S9, Supporting Information).[76] The hydrogen bond energy (ΔE_{HB}) at the modified position and interstrand stacking energy (ΔE_{inter}) at the hexa-nucleotide base pairs in which the modified nucleotides are in the middle were calculated (Figure S14, Supporting Information). The intrastrand stacking energy (ΔE_{intra}) was also calculated for trinucleotides in which the modified nucleotide is positioned in the middle. The ΔE_{HB} values at the modified nucleotides were higher than the bonding energy between two unmodified nucleotides (Table S9, Supporting Information). The same trends were observed in the case of ΔE_{intra}. The ΔE_{inter} was almost similar in guide strand modified, **3R-7R,** and unmodified, **3R-2R,** siRNAs. However, the siRNA duplex **6R-7R** containing modifications in the passenger and guide strand had higher ΔE_{inter} (Table S9, Supporting Information).

Taken together, MD analysis (20 ns) shows how the 4′-*C*-aminomethyl-2′-*O*-methyl modified nucleotides in the siRNA duplexes induce changes in the sugar puckering, flexibility in groove dimension, and disturbances in hydrogen bonding and base stacking when compared to the unmodified siRNA. This results in the slight decrease in the thermodynamic stability of the modified siRNA duplexes that was observed in the UV-melting studies.

■ CONCLUSIONS AND OUTLOOK

Syntheses of 4′-*C*-aminomethyl-2′-*O*-methyl uridine and cytidine nucleoside phosphoramidites and the corresponding siRNAs have been achieved. Thermal melting studies of modified siRNA showed a ~1 °C reduction in T_m per modification when compared to the unmodified duplexes. This modest destabilizing modification can perhaps be utilized to increase the thermodynamic asymmetry in siRNA duplexes, thereby enhancing their target specificity and potency.[20] Gene silencing studies in cellular systems showed that the 4′-*C*-aminomethyl-2′-*O*-methyl modification is compatible with the RNAi machinery, but the tolerance is position-dependent. The modifications are well tolerated at different positions in the passenger strand and at the 3′-end of the guide strand but less tolerated in the seed region of the guide strand. The decreased activity suggests that the 4′-*C*-aminomethyl group in the seed region is not optimally compatible with formation of an efficient RISC complex, possibly because of sterically unfavorable interactions with Ago2 protein. More structure−

activity studies replacing every nucleotide in the guide strands of siRNA are required to decipher complete positional tolerance of the modification.[77]

The presence of just two 4′-*C*-aminomethyl-2′-*O* methyl modifications in the siRNA guide strand resulted in higher serum stability compared to unmodified siRNA. This provides an opportunity to design siRNA containing a minimal number of modifications without sacrificing RNAi activity as well as nuclease stability. Minor groove base modifications are known to inhibit the off-target effects and immune stimulation.[78] Since the 4′-*C*-aminomethyl-2′-*O*-methyl modification projects into the minor groove, our modified siRNAs will be evaluated further for off-target and immune-stimulation effects. Since the effect of 4′-modifications on siRNA activity and off-target effects are rarely found in the literature, this modification provides an opportunity to unravel the structural and functional requirements of RNAi at the 4′-position. The 4′-*C*-aminomethyl groups can also be utilized to conjugate suitable molecules to siRNAs to enhance their *in vivo* delivery.[79,80]

MD simulations show that the overall structure of modified siRNA retains the A-type RNA helix with higher backbone flexibility and slight unwinding of the helices at the modified positions. The modification tunes the sugar puckering to C2′-endo *South*-type conformation, and the 4′-*C*-aminomethyl group has been found to have no significant interaction with the phosphate backbone. Modified siRNAs lose hydration in the minor groove; however, major groove and backbone hydration were retained when compared to the unmodified siRNA. We observed that hydrogen bonding and stacking energies were lower at the modified nucleotide positions in the siRNA. These local structure alterations result in lower thermodynamic stability of modified siRNA when compared to unmodified duplex, and indeed this was observed in our experimental studies. However, more structural studies are required to confirm the local conformational perturbations observed in the MD simulations. Our current modeling studies are directed toward deciphering the effect of this modification in the seed region of siRNA on RNAi by employing the siRNA-argonaute complexes. Overall, 4′-*C*-aminomethyl-2′-*O*-methyl modification is a potent RNAi-compatible chemical modification, which offers enhanced serum stability and therefore can further be evaluated for siRNA therapeutics.

■ EXPERIMENTAL SECTION

General. All chemicals and dry solvents (THF, MeOH, and DMF) were obtained from commercial sources and used without any further purification. Acetonitrile, DCM, Et$_3$N, DIPEA, and pyridine were dried using calcium hydride. Toluene was dried using calcium chloride. Thin layer chromatography (TLC) was performed on silica gel plates precoated with fluorescent indicator with visualization by UV light or by dipping into a solution of 5% (v/v) conc H$_2$SO$_4$ in ethanol and heating. Silica gel (100−200 mesh) was used for column chromatography. ^{1}H NMR (400 or 300 MHz), ^{13}C NMR (100 MHz), ^{31}P NMR (162 MHz), and ^{19}F NMR (376 or 282 MHz) were recorded on a 400 or 300 MHz instrument. The chemical shifts in parts per million (ppm) are reported downfield from TMS (0 ppm) or methanol-d_4 (3.31 ppm) for ^{1}H NMR spectra; CDCl$_3$ (77.2 ppm) or methanol-d_4 (49.1 ppm) for ^{13}C NMR spectra. Multiplicities of ^{1}H NMR spin couplings are reported as s for singlet, bs for broad singlet, d for doublet, t for triplet, q for quartet, sep for septet, dd for doublet of doublet, ABq for AB quartet, AXq for AX quartet, or m for multiplet and overlapping spin systems. Values for apparent coupling constants (*J*) are reported in Hz. High resolution mass spectra (HRMS) were obtained in positive ion electrospray ionization (ESI) mode. RNA sequences were synthesized using automated solid phase synthesizer

by employing standard phosphoramidite chemistry. Mass spectra of oligonucleotides were obtained in negative ESI mode.

1-[2′-*O*-Acetyl-3′,5′-di-*O*-benzyl-4′-*C*-azidomethyl-β-D-ribo-furanosyl]-uracil (5). Acetic anhydride (7.48 mL, 79.3 mmol) and acetic acid (40 mL) were added to compound 3 (2.6 g, 6.35 mmol). The mixture was cooled to 4 °C, and triflic acid (0.03 mL, 0.32 mmol) was added in dropwise. After stirring for 3 h at room temperature, the reaction mixture was quenched with cold saturated NaHCO$_3$ (60 mL) and extracted with ethyl acetate (3 × 150 mL). The organic layer was separated, dried over Na$_2$SO$_4$, and evaporated to give crude compound 4 (2 g, 4.7 mmol), which was co-evaporated with toluene (2 × 70 mL) and dried under high vacuum. The crude product 4 was dissolved in CH$_3$CN (47 mL). To this were added uracil (631 mg, 5.64 mmol) and *N,O*-bis(trimethylsilyl) acetamide (3.2 mL, 13.16 mmol), and the mixture was heated at 80 °C for 45 min until the suspension became a clear solution. This solution was cooled to 0 °C, and TMSOTf (1.1 mL, 6.11 mmol) was added in dropwise, warmed to 80 °C, and stirred overnight. The reaction was quenched with saturated NaHCO$_3$ solution (80 mL) and extracted with ethyl acetate (3 × 100 mL). The organic layer dried over Na$_2$SO$_4$, evaporated, and then purified by column chromatography (30−40% ethyl acetate in hexane) to yield compound 5 as white solid (1.88 g, 77%); R_f = 0.72 (70% ethyl acetate in pet ether); mp 123−124 °C; ^{1}H NMR (400 MHz, CDCl$_3$) δ 8.73 (bs, 1 H), 7.64 (d, *J* = 7.93 Hz, 1 H), 7.42−7.22 (m, 11 H), 6.18 (d, *J* = 4.8 Hz, 1 H) 5.40 (t, *J* = 5.18 Hz, 1 H), 5.34 (d, *J* = 8 Hz, 1 H), 4.63 (d, *J* = 11 Hz, 1 H), 4.49−4.41 (m, 3 H), 4.38 (d, *J* = 6 Hz, 1H), 3.77, 3.48 (AXq, *J* = 10.3 Hz, 2 H), 3.66, 3.36 (AXq, *J* = 13.4 Hz, 2 H), 2.12 (s, 3 H). ^{13}C NMR (100 MHz, CDCl$_3$) δ 170.0, 163.5, 150.5, 140.4, 137.1, 136.9, 128.8, 128.7, 128.5, 128.4, 128.3, 128.2, 102.8, 87.6, 87.5, 75.1, 74.6, 73.9, 71.2, 52.9, 20.7; HRMS (ESI) calcd for C$_{26}$H$_{28}$N$_5$O$_7$ [M + H]$^+$ 522.1989, found [M + H]$^+$ 522.1997 (Δ*m* +0.0008, error +1.6 ppm).

1-[2′-*O*-Acetyl-3′,5′-di-*O*-benzyl-4′-*C*-azidomethyl-β-D-ribo-furanosyl]-3-(4-methoxybenzyl)-uracil (6). To a mixture of compound 5 (3.65 g, 7 mmol) and 4-methoxybenzyl chloride (1.7 mL, 12.6 mmol) in CH$_3$CN (50 mL) was added DBU (1.95 mL, 14.03 mmol) at 0 °C, and the mixture was stirred at room temperature for 6 h. After cooling to 0 °C, the mixture was diluted with 5% KHSO$_4$ solution (10 mL). The organic phase was separated, and the aqueous phase was extracted with ethyl acetate (3 × 80 mL). The combined organic layer was washed with brine (100 mL), dried over anhydrous Na$_2$SO$_4$, and evaporated under reduced pressure to give a light yellow residue. Residue was purified by column chromatography (5−20% ethyl acetate in pet ether) to yield compound 6 as colorless oily liquid (4.0 g, 89%); R_f = 0.68 (40% ethyl acetate in pet ether); ^{1}H NMR (400 MHz, CDCl$_3$) δ 7.6 (d, *J* = 8.4 Hz, 1 H), 7.42−7.21 (m, 13 H), 6.82−6.79 (m, 2 H), 6.18 (d, *J* = 4.4 Hz, 1 H), 5.40−5.37 (m, 2 H), 5.04, 4.94 (ABq, *J* = 13.2 Hz, 2 H), 4.62, 4.43 (AXq, *J* = 11.6 Hz, 2 H), 4.44, 4.39 (ABq, *J* = 11.2 Hz, 2 H), 4.37 (d, *J* = 5.8 Hz, 1H), 3.75, 3.46 (AXq, *J* = 10.2 Hz, 2 H), 3.76 (s, 3 H), 3.66, 3.35 (AXq, *J* = 13.3 Hz, 2 H), 2.10 (s, 3 H); ^{13}C NMR (100 MHz, CDCl$_3$) δ 169.8, 162.5, 159.2, 151.1, 137.9, 137.2, 137.0, 130.7, 129.0, 128.8, 128.7, 128.6, 128.5, 128.4, 128.2, 128.2, 114.1, 113.8, 102.3, 88.3, 87.4, 77.1, 75.1, 74.5, 73.9, 71.1, 65.1, 55.4, 55.3, 52.9, 43.7, 20.8; HRMS (ESI) calcd for C$_{34}$H$_{36}$N$_5$O$_8$ [M + H]$^+$ 642.2564, found [M + H]$^+$ 642.2584 (Δ*m* +0.002, error +3.2 ppm).

1-[2′-*O*-Methyl-3′,5′-di-*O*-benzyl-4′-*C*-azidomethyl-β-D-ribo-furanosyl]-3-(4-methoxybenzyl)-uracil (8). Compound 6 (200 mg, 0.32 mmol) was dissolved in dry methanol (2 mL), to which 1 N NaOMe (0.57 mL) was added and stirred at room temperature for 3 h. The solvent was partially evaporated under reduced pressure and extracted with ethyl acetate (3 × 40 mL). The combined organic phase was washed with brine (40 mL), dried over anhydrous Na$_2$SO$_4$, and concentrated. The crude compound 7 obtained was co-evaporated with toluene (2 × 40 mL) and dried under high vacuum. Then compound 7 (146 mg, 0.24 mmol) was dissolved in dry THF (2 mL), and NaH (12 mg, 0.30 mmol) was added and stirred at 0 °C for 5 min. Then methyl iodide (0.02 mL, 0.35 mmol) was added in dropwise under nitrogen atmosphere and stirred at room temperature for 3 h. Saturated NaHCO$_3$ solution (50 mL) was added, the organic phase

was separated, and the aqueous phase was extracted with DCM (3 × 50 mL). The combined organic layer was washed with brine (40 mL), dried over anhydrous Na_2SO_4, and concentrated under reduced pressure. Crude residue was purified by column chromatography (12−14% ethyl acetate in pet ether) to afford **8** as yellow oily liquid (131 mg, 88%, after two steps); R_f = 0.83 (40% ethyl acetate in pet ether); ^{1}H NMR(400 MHz, $CDCl_3$) δ 7.87 (d, J = 7.6 Hz, 1 H), 7.43−7.18 (m, 13 H), 6.81 (d, J = 8.2 Hz, 2 H), 6.05 (d, J = 2 Hz, 1 H), 5.21 (d, J = 8.4 Hz, 1 H), 5.04, 4.94 (ABq, J = 13.6 Hz, 2 H), 4.70, 4.44 (AXq, J = 11.8 Hz, 2 H), 4.46, 4.40 (ABq, J = 10.9 Hz, 2 H), 4.26 (d, J = 5.6 Hz, 1 H), 3.95, 3.29 (AXq, J = 13.6 Hz, 2 H), 3.93, 3.52 (AXq, J = 10.4 Hz, 2H), 3.79−3.73 (m, 4 H), 3.57 (s, 3 H); ^{13}C NMR (100 MHz, $CDCl_3$) δ 162.6, 159.1, 150.7, 137.9, 137.2, 137.0, 130.7, 129.0, 128.7, 128.6, 128.4, 128.3, 128.1, 127.9, 113.7, 101.4, 89.2, 87.3, 83.6, 75.6, 73.7, 73.1, 70.0, 59.4, 55.3, 53.2, 43.5; HRMS (ESI) calcd for $C_{33}H_{36}N_5O_7$ $[M + H]^+$ 614.2615, found $[M + H]^+$ 614.2609 (Δm −0.0006, error −1.0 ppm).

1-[2′-O-Methyl-4′-C-trifluoroacetylaminomethyl-β-D-ribofuranosyl]-3-(4-methoxybenzyl)-5,6-dihydrouracil (9). Nucleoside **8** (1.5 g, 2.4 mmol) was dissolved in dry MeOH (39 mL). To this were added 20% Pd (OH)$_2$/C (2.19 g, 15.6 mmol) and ammonium formate (9.07 g, 144 mmol), and the reaction mixture was refluxed in H_2 atmosphere for 6 h. The reaction mixture was passed through a Celite pad, washed with MeOH (500 mL), concentrated under reduced pressure, and dried under high vacuum. The crude product was dissolved in dry MeOH (100 mL), to this solution were added CF_3COOEt (0.94 mL, 7.92 mmol) and Et_3N (1.83 mL, 13.2 mmol), and the mixture was stirred at room temperature overnight. The MeOH was evaporated under reduced pressure, and the residue was purified by column chromatography (2% MeOH in DCM) to afford sticky colorless compound **9** (680 mg, 71%); R_f = 0.51 (5% MeOH in DCM); ^{1}H NMR (400 MHz, $CDCl_3$) δ 7.37−7.27 (m, 4 H), 6.82 (d, J = 8.6 Hz, 2 H), 5.52 (d, J = 6.8 Hz, 1 H), 4.90, 4.85 (ABq, J = 14.0 Hz, 2 H), 4.40 (d, J = 5.6 Hz, 1 H), 4.18 (dd, J = 6.8 Hz, 5.8 Hz, 1 H), 3.78 (s, 3 H), 3.71−3.46 (m, 6 H), 3.44 (s, 3H), 2.76−2.72 (m, 2 H); ^{13}C NMR (100 MHz, $CDCl_3$) δ 168.9, 159.1, 158.5, 158.1, 153.9, 130.5, 129.6, 117.4, 114.6, 113.5, 90.3, 86.1, 80.1, 80.0, 71.0, 65.0, 58.9, 55.3, 43.6, 41.1, 38.8, 31.9. HRMS (ESI) calcd for $C_{21}H_{27}N_3O_8F_3$ $[M + H]^+$ 506.1750, found $[M + H]^+$ 506.1732 (Δm −0.0018, error −3.5 ppm).

1-[2′-O-Methyl-3′,5′-di-O-benzyl-4′-C-azidomethyl-β-D-ribofuranosyl]-uracil (10). Compound **8** (840 mg, 1.37 mmol) was dissolved in a CH_3CN/H_2O mixture (17 mL, v/v 9:1), and ceric ammonium nitrate (2.3 g, 5.5 mmol) was added. The reaction mixture was stirred at room temperature for 55 h. Saturated aqueous $NaHCO_3$ (100 mL) solution was added, and the mixture was stirred for an additional 20 min, then filtered, and extracted with CH_2Cl_2 (3 × 125 mL). The extract was dried over Na_2SO_4 and evaporated under reduced pressure. The residue was purified by column chromatography (40% ethyl acetate in pet ether) to give pale yellow oily compound **10** (517 mg, 76%); R_f = 0.26, (2% MeOH in DCM); ^{1}H NMR(300 MHz, $CDCl_3$) δ 9.22 (s, 1H), 7.93 (d, J = 7.8 Hz, 1 H), 7.39−7.20 (m, 11 H), 6.03 (d, J = 1.5 Hz, 1 H), 5.14 (d, J = 8.1 Hz, 1 H), 4.72, 4.46 (AXq, J = 11.7 Hz, 2 H), 4.49, 4.42 (ABq, J = 11.1 Hz, 2 H), 4.27 (d, J = 5.4 Hz, 1 H), 3.95, 3.31 (AXq, J = 13.6 Hz, 2 H), 3.96, 3.55 (AXq, J = 10.5 Hz, 2 H), 3.77 (dd, J = 5.5, 1.5 Hz, 1 H), 3.56 (s, 3H); ^{13}C NMR (100 MHz, $CDCl_3$) δ 163.6, 150.2, 140.4, 137.2, 137.1, 128.8, 128.7, 128.6, 128.5, 128.4, 128.3, 128.1, 101.8, 88.7, 87.6, 83.7, 75.6, 73.9, 73.2, 70.1, 59.5, 53.3; HRMS (ESI) calcd for $C_{25}H_{28}N_5O_6$ $[M + H]^+$ 494.2040, found $[M + H]^+$ 494.2060 (Δm +0.0021, error +4.2 ppm).

1-[2′-O-Methyl-3′,5′-di-O-benzyl-4′-C-trifluoroacetylaminomethyl-β-D-ribofuranosyl]-uracil (11). Nucleoside **10** (1.1 g, 2.23 mmol) was dissolved in THF (23 mL). To this were added water (0.2 mL) and PPh_3 (1.17 g, 4.46 mmol). The reaction mixture was heated at 45 °C for 4 h and then cooled to 0 °C. Then CF_3COOEt (1.33 mL, 11.15 mmol) and Et_3N (1.55 mL, 11.15 mmol) were added, and the reaction mixture was stirred at room temperature for overnight. The solvent was evaporated under reduced pressure and co-evaporated with toluene (2 × 40 mL). The crude compound was purified by column chromatography (40% ethyl acetate in pet ether) to afford

gummy colorless compound **11** (1.268 g, 100%); R_f = 0.58, (40% ethyl acetate in pet ether); ^{1}H NMR (300 MHz, CD_3OD) δ 7.93 (d, J = 8.1 Hz, 1 H), 7.38−7.21 (m, 11 H), 6.04 (d, J = 0.9 Hz, 1 H), 5.11 (d, J = 8.1 Hz, 1 H), 4.71, 4.49 (AXq, J = 11.7 Hz, 2 H), 4.44, 4.38 (ABq, J = 10.9 Hz, 2 H), 4.42 (d, J = 5.9 Hz, 1 H), 3.98 (dd, J = 5.7 Hz, 0.9 Hz, 1H), 3.83, 3.61 (ABq, J = 14.5 Hz, 2 H), 3.68, 3.56 (ABq, J = 10.7 Hz, 2 H), 3.55 (s, 3 H); ^{13}C NMR (75.4 MHz, CD_3OD) δ 166.1, 159.44, 151.7, 142.4, 138.9, 138.8, 133.8, 133.8, 133.4, 133.2, 133.1, 132.0, 130.1, 129.9, 129.6, 129.5, 129.3, 129.2, 129.2, 119.5, 115.7, 102.1, 90.6, 88.3, 84.3, 77.0, 74.6, 73.8, 71.1, 59.5, 42.7; ^{19}F NMR (282 MHz, CD_3OD) δ −76.2 (s); HRMS (ESI) calcd for $C_{27}H_{29}F_3N_3O_7$ [M + H]$^+$ 564.1958, found $[M + H]^+$ 564.1973 (Δm +0.0016, error +2.8 ppm).

1-[2′-O-Methyl-4′-C-trifluoroacetylaminomethyl-β-D-ribofuranosyl]-uracil (12). Compound **11** (3.5 g, 6.21 mmol) was dissolved in EtOH (106 mL), and then 10% Pd/C (1.5 g) was added and heated at 70 °C for 16 h under H_2 atmosphere. The reaction mixture was filtered through Celite pad and washed with MeOH (600 mL). The MeOH layer was evaporated and purified by column chromatography (5% MeOH in DCM) to give **12** as a white solid (1.65 g, 71%); R_f = 0.24, (5% MeOH in DCM); mp 124−126 °C; ^{1}H NMR (300 MHz, CD_3OD) δ 8.04 (d, J = 8.1 Hz, 1H), 6.05 (d, J = 4.2 Hz, 1H), 5.7 (d, J = 8.1 Hz, 1H), 4.51 (d, J = 5.7 Hz, 1H), 4.02 (dd, J = 5.7 Hz, 4.8 Hz, 1H), 3.67, 3.59 (ABq, J = 14.1 Hz, 2H), 3.65, 3.60 (ABq, J = 12.2 Hz, 2H), 3.51 (s, 3H); ^{13}C NMR (75 MHz, CD_3OD) δ 166.2, 159.5, 152.2, 142.8, 119.5, 115.7, 102.9, 89.2, 85.2, 71.2, 64.3, 59.3, 42.1; ^{19}F NMR (282 MHz, CD_3OD) δ −76.1; HRMS (ESI) calcd for $C_{13}H_{17}F_3N_3O_7$ $[M + H]^+$ 384.1019, found $[M + H]^+$ 384.1028 (Δm +0.0009, error +2.6 ppm).

1-[2′-O-Methyl-4′-C-trifluoroacetylaminomethyl-5′-O-(4,4′-dimethoxytrityl)-β-D-ribofuranosyl]-uracil (13). Compound **12** (200 mg, 0.52 mmol) was co-evaporated with dry pyridine (2 × 10 mL) and redissolved in the same solvent (8 mL). DMT-Cl (352 mg, 1.04 mmol) was added and stirred at room temperature for 24 h. A saturated solution of $NaHCO_3$ (50 mL) was added and extracted with DCM (3 × 80 mL). The organic layer was dried over Na_2SO_4, filtered, and evaporated under reduced pressure. The residue was purified by column chromatography (60% ethyl acetate in pet ether + 2% Et_3N) to give **13** as pale yellow solid (287 mg, 81%); R_f = 0.3, (60% ethyl acetate in pet ether + 2% Et_3N); mp 122−123 °C; ^{1}H NMR (400 MHz, $CDCl_3$) δ 7.61 (d, J = 8.1 Hz, 1H), 7.36− 7.23 (m, 10H), 7.09 (t, J = 5.8 Hz, 1H), 6.83 (d, J = 8.9 Hz, 4H), 6.04 (d, J = 4.2 Hz, 1H), 5.36 (d, J = 8.1 Hz, 1H), 4.52 (d, J = 6 Hz, 1H), 4.04 (dd, J = 5.7 Hz, 4.5 Hz, 1H), 3.79 (s, 6H), 3.64 (d, J = 6 Hz, 2H), 3.55 (s, 3H), 3.42, 3.32 (ABq, J = 10.7 Hz, 2 H); ^{13}C NMR (100 MHz, $CDCl_3$) δ 163.4, 159.0, 157.7, 150.4, 143.9, 140.3, 134.8, 134.6, 130.2, 128.3, 128.2, 127.5, 116, 113.5, 103.0, 87.9, 87.3, 83.8, 71.2, 65.6, 59.5, 55.2, 41.3; ^{19}F NMR (282 MHz, CD_3OD) δ −75.4 (s); HRMS (ESI) calcd for $C_{34}H_{35}F_3N_3O_9$ $[M + H]^+$ 686.2325, found $[M + H]^+$ 686.2354 (Δm +0.0028, error +4.1 ppm).

1-{2′-O-Methyl-3′-O-[2-cyanoethoxy(diisopropylamino)-phosphino]-4′-C-trifluoroacetylaminomethyl-5′-O-(4,4′-dimethoxytrityl)-β-D-ribofuranosyl}-uracil (14). Compound **13** (150 mg, 0.22 mmol) was dissolved in DCM (3 mL). To this were added DIPEA (0.3 mL, 1.74 mmol) and CEP-Cl (0.15 mL, 0.65 mmol), and the mixture was stirred at room temperature for 75 min. Then MeOH (0.5 mL) was added and stirred for 15 min. The reaction mixture was diluted with DCM (100 mL), washed with $NaHCO_3$ (3 × 50 mL), dried over Na_2SO_4, and evaporated under reduced pressure. The crude compound was purified by column chromatography (50−60% DCM in pet ether) to give **14** as a white solid (130 mg, 70%); R_f = 0.7 (8% MeOH in DCM + 2% Et_3N); mp 80−81 °C; ^{31}P NMR (162 MHz, $CDCl_3$) δ 151.40, 151.16; ^{19}F NMR (282 MHz, $CDCl_3$) δ −75.82, −75.98; HRMS (ESI) calcd for $C_{43}H_{52}N_5O_{10}F_3P$ $[M + H]^+$ 886.3404, found $[M + H]^+$ 886.3401 (Δm −0.0003, error −0.3 ppm).

1-[2′-O-Methyl-4′-C-trifluoroacetylaminomethyl-5′-O-(4,4′-dimethoxytrityl)-β-D-ribofuranosyl]-cytosine (17). Nucleoside **13** (50 mg, 0.073 mmol) was dissolved in dry pyridine (2 mL). To this was added Ac_2O (0.03 mL, 0.36 mmol), and the mixture was stirred at room temperature overnight. Then, $NaHCO_3$ (30 mL) was added and

extracted with EtOAc (3 × 60 mL). The EtOAc layer was dried over Na$_2$SO$_4$, evaporated followed by co-evaporation with toluene (20 mL), and dried under high vac to give crude compound **15**. Compound **15** (50 mg, 0.073 mmol) was dissolved in DCM (1.5 mL) in an ice bath, and then DMAP (1 mg, 0.008 mmol), Et$_3$N (0.1 mL, 0.73 mmol) and 2,4,6-triisopropylbenzenesulphonylchloride (33 mg, 0.11 mmol) were added. The reaction mixture was stirred at room temperature for 6 h. Then the reaction mixture was diluted with DCM (70 mL), washed with saturated NaHCO$_3$ (3 × 60 mL), dried over Na$_2$SO$_4$, and evaporated under reduced pressure. The crude compound **16** obtained was dissolved in THF (1.6 mL), then aq NH$_3$ (0.3 mL) was added at 0 °C, and the mixture was stirred at room temperature for overnight. The reaction mixture was evaporated and purified by column chromatography (5% MeOH in DCM + 2% Et$_3$N) to give nucleoside **17** as pale yellow solid (31 mg, 63%, after 3 steps); R_f = 0.35 (4% MeOH in DCM + 2% Et$_3$N); mp 124–126 °C; ^{1}H NMR(400 MHz, CD$_3$OD) δ 7.97 (d, J = 7.5 Hz, 1H), 7.41 (m, 2 H), 7.35–7.24 (m, 7H), 6.86 (d, J = 8.5 Hz, 4H), 6.04 (d, J = 2.3 Hz, 1H), 5.43 (d, J = 7.4 Hz, 1H), 4.71 (d, J = 6 Hz, 1H), 3.88 (dd, J = 6 Hz, 2.5 Hz, 1H), 3.77 (s, 6H), 3.69, 3.62 (ABq, J = 14.0 Hz, 2 H), 3.57 (s, 3H), 3.49–3.44 (m, 2H); ^{13}C NMR (100 MHz, CD$_3$OD) δ 167.7, 160.4, 160.3, 157.9, 145.9, 143.0, 136.7, 136.4, 131.6, 131.5, 129.5, 129.0, 128.2, 116.9, 114.3, 114.3, 96.1, 90.7, 88.7, 88.5, 86.0, 71.4, 65.0, 59.7, 55.8, 53.8, 42.4; ^{19}F NMR (282 MHz, CD$_3$OD) δ −77.0; HRMS (ESI) calcd for C$_{34}$H$_{36}$N$_4$O$_8$F$_3$ [M + H]$^+$ 685.2485, found [M + H]$^+$ 685.2485, (Δm 0.0, error 0.0 ppm).

1-[2′-O-Methyl-4′-C-trifluoroacetylaminomethyl-5′-O-(4,4′-dimethoxytrityl)-β-D-ribofuranosyl]-N^4-(isobutyryl)-cytosine (18). Nucleoside **17** (70 mg, 0.10 mmol) was dissolved in dry pyridine (2 mL). Then trimethylsilyl chloride (0.06 mL, 0.51 mmol) was added dropwise at 0 °C and stirred at room temperature for 45 min. Isobutyryl chloride (0.02 mL, 0.20 mmol) was added at 0 °C and stirred for 4 h. After completion of reaction, dry MeOH (0.5 mL) was added and stirred for 20 min. Saturated NaHCO$_3$ solution (50 mL) was added and extracted with DCM (3 × 60 mL). The organic layer was dried over Na$_2$SO$_4$ and evaporated under reduced pressure. The crude compound was purified by column chromatography (2% MeOH in DCM + 2% Et$_3$N) to give **18** as white solid (50 mg, 67%); R_f = 0.44 (3–4% MeOH in DCM + 2% Et$_3$N); mp 164–166 °C; ^{1}H NMR (400 MHz, CDCl$_3$) δ 8.66 (bs, 1H), 8.06 (d, J = 7.5 Hz, 1H), 7.38–7.23 (m, 9H), 7.10 (d, J = 7.5 Hz, 1H), 6.85–6.81 (m, 4H), 6.08 (d, J = 2.2 Hz, 1H), 4.50 (d, J = 6.1 Hz, 1H), 3.99–3.93 (m, 1H), 3.80 (s, 6H), 3.78–3.66 (m, 2H), 3.64 (s, 3H), 3.44, 3.38 (ABq, J = 10.7 Hz, 2H), 2.60 (sep, J = 6.8 Hz, 1H), 1.20 (d, J = 6.8 Hz, 3H); 1.19 (d, J = 6.8 Hz, 3H); ^{13}C NMR (100 MHz, CDCl$_3$) δ 177.1, 162.8,158.9, 157.7, 157.5, 155.2, 144.7, 143.8, 135.2, 134.8, 130.3, 130.1, 128.3, 128.2, 127.5, 116, 113.6, 97.0, 89.9, 87.7, 87.7, 84.6, 70.8, 65.2, 59.8, 55.4, 41.2, 36.7, 19.2, 19.1; ^{19}F NMR (376 MHz, CDCl$_3$) δ −75.82; HRMS (ESI) calcd for C$_{38}$H$_{42}$N$_4$O$_9$F$_3$ [M + H]$^+$ 755.2904, found [M + H]$^+$ 755.2905 (Δm +0.0001, error +0.1 ppm).

1-{2′-O-Methyl-3′-O-[2-cyanoethoxy(diisopropylamino)-phosphino]-4′-C-trifluoroacetylaminomethyl-5′-O-(4,4′-dimethoxytrityl-β-D-ribofuranosyl}-N^4-(isobutyryl)-cytosine (19). The compound **18** (50 mg, 0.06 mmol) was dissolved in DCM (1.2 mL). Then DIPEA (0.09 mL, 0.52 mmol) and CEP-Cl (0.04 mL, 0.2 mmol) were added and stirred at room temperature for 40 min. After completion of reaction, dry MeOH (0.05 mL) was added and stirred for 15 min. The reaction mixture was diluted with DCM (100 mL), washed with saturated NaHCO$_3$ (3 × 50 mL), dried over Na$_2$SO$_4$, and evaporated under reduced pressure. The crude compound was purified by column chromatography (60% DCM in pet ether) to give **19** as white solid (35 mg, 51%); R_f = 0.88 (4% MeOH in DCM + 2% Et$_3$N); mp 94–95 °C; ^{31}P NMR (162 MHz, CDCl$_3$) δ 151.18, 151.10; ^{19}F NMR (282 MHz, CDCl$_3$) δ −76.25, −76.31; HRMS (ESI) calcd for C$_{47}$H$_{59}$N$_6$O$_{10}$F$_3$P [M + H]$^+$ 955.3982, found [M + H]$^+$ 955.4011 (Δm +0.0028, error +3.0 ppm).

RNA Synthesis and Purification. The unmodified and modified siRNA sequences were synthesized on 0.2 μmol scale on an automated DNA/RNA synthesizer using standard CPG solid support. The coupling time used for modified uridine and cytidine phosphoramidite

was 10 min, and for unmodified amidite (2′-O-TBMDS protected) it was 6.5 min. 5-Ethylthio-1H-tetrazole (ETT) was used as coupling agent. After the synthesis, the CPG beads were treated with the 400 μL of 10% diethyl amine in anhydrous acetonitrile to selectively remove cyanoethyl groups. Then the beads were washed with acetonitrile (2 × 400 μL). The supernatant was removed, and the support was dried under desiccant mode in speed vac. The cleavage from support and deprotection of base protecting groups were carried out by treating the beads with 1 mL of 41% methylamine in water and 30% aq NH$_3$ (1:1 v/v) for 18 min at 65 °C. Supernatant was collected, and the support was washed with 1:1 mixture (300 μL) of EtOH and water. The combined fractions were evaporated on a vacuum concentrator. To remove 2′-O-TBDMS groups, oligonucleotides were dissolved in 100 μL of dry DMSO, and 125 μL of Et$_3$N·3HF was added and heated at 65 °C for 2.5 h. The Et$_3$N·3HF was quenched with the addition of 400 μL of isopropyl trimethyl silyl ether, and RNA was precipitated twice by adding 850 μL of cold diethyl ether. RNA was recovered by centrifugation at 16,100 RCF for 10 min at 4 °C. The RNA pellet was dried in the desiccant mode in a vacuum concentrator for 20 min. The crude RNA was dissolved in water and purified by 20% denaturing PAGE (7 M urea) at 30 W using 1× TBE buffer (89 mM each Tris HCl and boric acid and 2 mM EDTA, pH 8.3). The gel was visualized, and bands were marked under UV lamp. The desired gel band was excised and crushed, 15 mL of TEN (10 mM Tris, 1 mM EDTA, 300 mM NaCl pH 8.0) was added, and the mixture was shaken for 16 h at room temperature for the recovery. The RNA samples were desalted using a Sep-Pak (C-18) column. After evaporation, the RNA pellet was dissolved in water, and the concentration was measured at 260 nm in a UV−vis spectrophotometer using appropriate molar extinction coefficients (ε).

Thermal Melting Experiments. Melting temperature analysis was carried out by measuring change in absorbance at 260 nm with increase in temperature using a UV spectrophotometer coupled with a peltier controller. Duplexes were prepared using equimolar concentration (1 μM) of complementary strands in a buffer solution containing 100 mM NaCl, 10 mM Na$_2$PO$_4$ pH 7.4, 0.1 mM EDTA. The solution containing passenger strand and guide strands was heated at 95 °C for 2 min, then gradually cooled to room temperature, and stored at 4 °C. Before the measurements, samples were equilibrated at 25 °C for 10 min and then heated to 95 °C in an increment of 0.5 °C/min. The change in absorbance against increase in temperature was recorded, and T_m was calculated utilizing the first order derivative method. All experiments were triplicated, and the T_m values reported are average of 3 measurements.

Cell Culture and Gene Silencing Studies. HeLa cells were grown in Eagle's minimum essential media (MEM) supplemented with 10% heat inactivated fetal bovine serum (FBS) and the antibiotics penicillin (100 units/mL) and streptomycin (100 units/mL) at 37 °C in 5% CO$_2$ environment. Twenty-four hours prior to transfection, cells were plated in 24-well plates at a density of 3 × 10^5 cells/well. Before transfection, the media was removed, and cells were washed with phosphate buffered saline (PBS; 137 mM NaCl, 27 mM KCl, 10 mM Na$_2$HPO$_4$, 2 mM KH$_2$PO$_4$, pH 7.4). The cells were transfected with siRNA (33 nM, 10 pmol/well) in serum-free media. The cells were cotransfected with psiCHECK2 plasmid (0.08 nM, 100 ng/well); 1.5 μL (1 μg/μL) of Lipofectamine-2000 was used for the transfection, and the protocols detailed in the Lipofectamine-2000 manual were followed. The cells were incubated for 5 h, and media was replaced with fresh media containing 20% FBS without antibiotics. Then after 12 h, the media was changed with fresh media containing 20% FBS with antibiotics. After 48 h post transfection, media was removed, and the cells were washed with PBS and then lysed using passive lysis buffer. The cell lysate was used for dual luciferase assay system and gene expression measured using luminometer. The ratio between relative light units of *Renilla* and *Firefly* luciferase was determined for each well and normalized using the value obtained from positive control experiments (no siRNA). The luminescence values reported are an average of four independent experiments. Statistical analyses between individual groups were performed by a Student t test; a P value of <0.05 was considered statistically significant.

5′-End Radiolabeling of Oligonucleotides. Twenty-five picomoles of RNA was mixed with PNK enzyme (5 units) and γ-^{32}P ATP (10 μCi) in PNK buffer (50 mM Tris-HCl, 10 mM MgCl$_2$, 5 mM DTT, 0.1 mM each spermidine and EDTA, pH 7.6) with a final volume of 10 μL. The reaction mixture was incubated at 37 °C for 1 h. The enzyme was deactivated by the addition of 10 μL of stop solution (80% formamide, 50 mM EDTA, 0.025% of each bromophenol blue and xylene cyanol). The labeled oligonucleotides were purified by 20% denaturing PAGE (7 M urea), extracted with TEN, and precipitated using ethanol.

Serum Stability Assay. ^{32}P-Labeled guide strands (0.15 μM) were mixed with excess cold complementary unmodified passanger strands (1 μM) in PBS. The solutions were heated at 95 °C for 2 min and then gradually cooled to room temperature. The annealed siRNA duplexes were incubated at 25 °C in 10% human serum (from male AB clotted whole blood) in PBS with a final volume of 10 μL. The aliquots of 1 μL were withdrawn after 0 min, 15 min, 30 min, 1 h, 2 h, 4 h, 8 h, 22 h, and 44 h, quenched with 4 μL of stop solution (80% formamide, 50 mM EDTA, 0.025% of each bromophenol blue and xylene cyanol), and stored at −20 °C. The samples were analyzed on 20% denaturing PAGE (7 M urea). Gels were visualized by using a phosphorimager.

Molecular Modeling Studies. The starting structures of three isosequential siRNA duplexes (**3R-2R, 3R-7R,** and **6R-7R**) with modifications at different positions were modeled using the NUCGEN module implemented in AMBER 10.[54] The force field parameters for the modified nucleotides were obtained using the protocol developed by Aduri and co-workers,[81] and RESP charges were derived using Antechamber RESP fitting procedure developed by Kollman and co-workers.[82] Unmodified uridine nucleotide at respective positions were replaced by 4′-C-aminomethyl-2′-O-methyl modified uridine using the calculated parameters, and charges by XLeap module in AMBER 10.

Each duplex was immersed in an octahedron-shaped box containing ~4500 TIP3P water molecules extended up to 10 Å away from any of the solute atom. Forty-one sodium ions were randomly added to neutralize the charge of the phosphate backbone. All of the simulations reported here were performed using the SANDER module of AMBER 10. After solvation, the system was then subjected to an equilibration protocol involving 2500 steps of steepest descent minimization of solvent, and 2500 steps of conjugate gradient, holding the solute/RNA duplex to their initial position by means of positional restraints. Further minimization was carried for the whole system by 5000 steps of conjugate gradient method without any positional restraints, allowing the system to attain relaxed geometry. Then the solvent was heated from 0 to 300 K, with 10 kcal/(mol Å^2) constraints for RNA duplex in a period of 100 ps keeping a constant volume. Next the equilibration was continued to 200 ps at a constant pressure (1 atm) and temperature (300 ± 10 K). Constant temperature was maintained using a Langvein algorithm. After equilibration, systems were subjected to 20 ns of MD simulation saving trajectory coordinates for each picosecond. All covalent bonds involving hydrogen atoms were constrained using SHAKE.[83] Long range interactions were treated using the particle mesh Ewald method,[84] and the cut-off distance was set to10 Å for Lennard−Jones potential.

Trajectory analysis was done using the Ptraj module in AMBER 10, X3DNA program,[85] in-house programs and examined visually using VMD 1.4.6.[86] The rotational and translational motions were removed from trajectories by superimposing the siRNA duplex to their starting structure. The root-mean-square deviation (rmsd) values were calculated over 20 ns MD simulation for all heavy atoms in each duplex with respect to their corresponding reference structure. The rmsd values were also calculated for the regions containing modified nucleotides flanked by one base pair on either side along with their complementary residues. The interstrand phosphate distance was calculated as the distance between the phosphorus atom of a nucleotide in one strand and phosphorus atom of a nucleotide in the partner strand, and the intrastrand phosphate distance as the distance between phosphorus atoms in two successive nucleotides within a strand. The root-mean-square fluctuation (rmsf) values were calculated around average structures for the heavy atoms composing the backbone (C3′, O3′, P, O1P, O2P, C5′ and O5′) of each nucleotide.

The percentage of occurrence of C3′-endo sugar conformation during MD simulation at each nucleotide in both strands of all of the duplexes were calculated using the X3DNA program. The amplitude of the pseudo rotational angle (*tm*), which represents the four dihedral angles with their distribution, was determined for each nucleotide in all duplexes using the X3DNA program. Water density or hydration numbers, which represent the average number of water molecules present in a distance of less than 3.0 Å from solute atoms over 20 ns, were computed for major groove, minor groove and backbone atoms separately using Ptraj module in AMBER 10. The helicoidal deformation parameters (buckle, open angle, propeller, stagger, shear, stretch)[87] and base pair step parameters (shift, slide, roll, rise, tilt, twist)[88] were calculated for each dinucleotide steps of all of the duplexes by the X3DNA program. The distribution of χ angle at the modified nucleotide level was calculated using the Ptraj module and fit to normalize Gaussian. The percentages of occupancies of two Watson−Crick hydrogen bonds between A-U base pair at the modified position were also determined over 20 ns simulation using Ptraj module.

The stacking and hydrogen bond interaction energies at the modified regions were computed at the MP2(full)/6-311G* level using the Gaussian03 program.[53] The interaction energy was categorized into hydrogen bond energy (ΔE_{HB}), interstrand stacking energy (ΔE_{inter}), and intrastrand stacking energy (ΔE_{intra}). Stacking energies were calculated solely based upon the electrostatic and van der Waals interaction, which were calculated using Molecular Mechanics with AMBER FF03[89] and Lennard−Jones (6−12) potential. Basis set superposition error (BSSE) for hydrogen bonds energy and stacking interactions were corrected using the counterpoise method.[90] All of the structures were visualized, and the figures were rendered using PyMOL v0.99 (http://www.pymol.org).

■ ASSOCIATED CONTENT

⑤ Supporting Information

Thermal melting plots for modified siRNAs, additional data from molecular modeling studies, ESI-MS data for oligonucleotides, and copies of NMR spectra of all the new compounds. This material is available free of charge via the Internet at http://pubs.acs.org.

■ AUTHOR INFORMATION

Corresponding Author
*E-mail: pradeep@chem.iitb.ac.in.

Notes
The authors declare no competing financial interest.

■ ACKNOWLEDGMENTS

■ REFERENCES

(1) Fire, A.; Xu, S. Q.; Montgomery, M. K.; Kostas, S. A.; Driver, S. E.; Mello, C. C. *Nature* **1998**, *391*, 806–811.

(2) Elbashir, S. M.; Harborth, J.; Lendeckel, W.; Yalcin, A.; Weber, K.; Tuschl, T. *Nature* **2001**, *411*, 494–498.

(3) Zamore, P. D.; Tuschl, T.; Sharp, P. A.; Bartel, D. P. *Cell* **2000**, *101*, 25–33.

(4) Kawamata, T.; Tomari, Y. *Trends Biochem. Sci.* **2010**, *35*, 368–376.

(5) Filipowicz, W. *Cell* **2005**, *122*, 17–20.

(6) Castanotto, D.; Rossi, J. J. *Nature* **2009**, *457*, 426–433.

(7) Davidson, B. L; McCray, P. B. *Nat. Rev. Genet.* **2011**, *12*, 329–340.

(8) Shukla, S.; Sumaria, C. S.; Pradeepkumar, P. I. *ChemMedChem.* **2010**, *5*, 328–349.

(9) Turner, J. J.; Jones, S. W.; Moschos, S. A.; Lindsay, M. A.; Gait, M. J. *Mol. Biosyst.* **2007**, *3*, 43–50.

(10) Jackson, A. L.; Linsley, P. S. *Nat. Rev. Drug Discovery* **2010**, *9*, 57–67.

(11) Jackson, A. L.; Burchard, J.; Schelter, J.; Chau, B. N.; Cleary, M.; Lim, L.; Linsley, P. S. *RNA* **2006**, *12*, 1179–1187.

(12) Hartmann, G. *J. Clin. Invest.* **2009**, *119*, 438–441.

(13) Whitehead, K. A.; Langer, R.; Anderson, D. G. *Nat. Rev. Drug Discovery* **2009**, *8*, 129–138.

(14) Watts, J. K.; Deleavey, G. F.; Damha, M. J. *Drug Discovery Today* **2008**, *13*, 842–855.

(15) Behlke, M. A. *Oligonucleotides* **2008**, *18*, 305–320.

(16) Phelps, K.; Morris, A.; Beal, P. A. *ACS Chem. Biol.* **2012**, *7*, 100–109.

(17) Prakash, T. P.; Allerson, C. R.; Dande, P.; Vickers, T. A.; Sioufi, N.; Jarres, R.; Baker, B. F.; Swayze, E. E.; Griffey, R. H.; Bhat, B. *J. Med. Chem.* **2005**, *48*, 4247–4253.

(18) Manoharan, M.; Akinc, A.; Pandey, R. K.; Qin, J.; Hadwiger, P.; John, M.; Mills, K.; Charisse, K.; Maier, M. A.; Nechev, L.; Greene, E. M.; Pallen, P. S.; Rozners, E.; Rajeev, K. G.; Egli, M. *Angew. Chem., Int. Ed.* **2011**, *50*, 2284–2288.

(19) Veedu, R. N.; Wengel, J. *Chem. Biodiversity* **2010**, *7*, 536–542.

(20) Bramsen, J. B.; Laursen, M. B.; Nielsen, A. F.; Hansen, T. B.; Bus, C.; Langkjær, N.; Babu, B. R.; Højland, T.; Abramov, M.; Van Aerschot, A.; Odadzic, D.; Smicius, R.; Haas, J.; Andree, C.; Barman, J.; Wenska, M.; Srivastava, P.; Zhou, C.; Honcharenko, D.; Hess, S.; Müller, E.; Bobkov, G. V.; Mikhailov, S. N.; Fava, E.; Meyer, T. F.; Chattopadhyaya, J.; Zerial, M.; Engels, J. W.; Herdewijn, P.; Wengel, J.; Kjems, J. *Nucleic Acids Res.* **2009**, *37*, 2867–2881.

(21) Zhou, C.; Chattopadhyaya., J. *Curr. Opin. Drug Discovery Dev.* **2009**, *12*, 876–898.

(22) Dowler, T.; Bergeron, D.; Tedeschi, A. L.; Paquet, L.; Ferrari, N.; Damha, M. J. *Nucleic Acids Res.* **2006**, *34*, 1669–1675.

(23) Fauster, K.; Hartl, M.; Santner, T.; Aigner, M.; Kreutz, C.; Bister, K.; Ennifar, E.; Micura, R. *ACS Chem. Biol.* **2012**, DOI: DOI: 10.1021/cb200510k.

(24) Detzer, A.; Overhoff, M.; Mescalchin, A.; Rompf, M.; Sczakiel, G. *Curr. Pharm. Des.* **2008**, *14*, 3666–3673.

(25) Hall, A. H.; Wan, J.; Spesock, A.; Sergueeva, Z.; Shaw, B. R.; Alexander, K. A. *Nucleic Acids Res.* **2006**, *34*, 2773–2781.

(26) Terrazas, M.; Kool, E. T. *Nucleic Acids Res.* **2009**, *37*, 346–353.

(27) Kannan, A.; Fostvedt, E.; Beal, P. A.; Burrows, C. J. *J. Am. Chem. Soc.* **2011**, *133*, 6343–6351.

(28) Peacock, H.; Kannan, A.; Beal, P. A.; Burrows, C. J. *J. Org. Chem.* **2011**, *76*, 7295–7300.

(29) Lima, W. F.; Wu, H.; Nichols, J. G.; Sun, H.; Murray, H. M.; Crooke, S. T. *J. Biol. Chem.* **2009**, *284*, 26017–26028.

(30) Takahashi, M.; Minakawa, N.; Matsuda, A. *Nucleic Acids Res.* **2009**, *37*, 1353–1362.

(31) Watts, J. K.; Choubdar, N.; Sadalapure, K.; Robert, F.; Wahba, A. S.; Pelletier, J.; Pinto, B. M.; Damha, M. J. *Nucleic Acids Res.* **2007**, *35*, 1441–1451.

(32) Pfundheller, H. M.; Wengel, J. *Bioorg. Med. Chem. Lett.* **1999**, *9*, 2667–2672.

(33) Pfundheller, H. M.; Bryld, T.; Olsen, C. E.; Wengel, J. *Helv. Chim. Acta* **2000**, *83*, 128–151.

(34) Sioud, M. *Eur. J. Immunol.* **2006**, *36*, 1222–1230.

(35) Chiu, Y. L.; Rana, T. M. *RNA* **2003**, *9*, 1034–1048.

(36) Debart, F.; Abes, S.; Deglane, G.; Moulton, H. M.; Clair, P.; Gait, M. J.; Vasseur, J. J.; Lebleu, B. *Curr. Top. Med. Chem.* **2007**, *7*, 727–737.

(37) Griffey, R. H.; Monia, B. P.; Cummins, L. L.; Freier, S.; Greig, M. J.; Guinosso, C. J.; Lesnik, E.; Manalili, S. M.; Mohan, V.; Owens, S.; Ross, B. R.; Sasmor, H.; Wancewicz, E.; Weiler, K.; Wheeler, P. D.; Cook, P. D. *J. Med. Chem.* **1996**, *39*, 5100–5109.

(38) Kanazaki, M.; Ueno, Y.; Shuto, S.; Matsuda, A. *J. Am. Chem. Soc.* **2000**, *122*, 2422–2432.

(39) Youssefyeh, R. D.; Verheyden, J. P. H; Moffatt, J. G. *J. Org. Chem.* **1979**, *44*, 1301–1309.

(40) Koshkin, A. A.; Singh, S. K.; Nielsen, P.; Rajwanshi, V. K.; Kumar, R.; Meldgaard, M.; Olsen, E.; Wengel, J. *Tetrahedron* **1998**, *54*, 3607–3630.

(41) Varghese, O. P.; Barman, J.; Pathmasiri, W.; Plashkevych, O; Honcharenko, D.; Chattopadhyaya, J. *J. Am. Chem. Soc.* **2006**, *128*, 15173–15187.

(42) Akiyama, T.; Nishimoto, H.; Ozaki, S. *Bull. Chem. Soc. Jpn.* **1990**, *63*, 3356–3357.

(43) Honcharenko, D.; Varghese, O. P.; Plashkevych, O.; Barman, J; Chattopadhyaya, J. *J. Org. Chem.* **2006**, *71*, 299–314.

(44) Kumar, T. S.; Kumar, P.; Sharma, P. K.; Hrdlicka, P. J. *Tetrahedron Lett.* **2008**, *49*, 7168–7170.

(45) Jin, S.; Miduturu, C. V.; McKinney, D. C.; Silverman, S. K. *J. Org. Chem.* **2005**, *70*, 4284–4299.

(46) Hobartner, C.; Kreutz, C.; Flecker, E.; Ottenschlaeger, E.; Pils, W.; Grubmayr, K.; Micura, R. *Monatsh. Chem.* **2003**, *134*, 851–873.

(47) Hobartner, C.; Micura, R. *J. Am. Chem. Soc.* **2004**, *126*, 1141–1149.

(48) Reddy, M. P.; Hanna, N. B.; Farooqui, F. *Tethedron Lett.* **1994**, *35*, 4311–4314.

(49) Song, Q.; Jones, R. A. *Tetrahedron Lett.* **1999**, *40*, 4653–4654.

(50) Inoue, H.; Hayase, Y.; Imura, A.; Iwai, S.; Miura, K.; Ohtsuka, E. *Nucleic Acids Res.* **1987**, *15*, 6131–6148.

(51) Wang, Y.; Sheng, G.; Juranek, S.; Tuschl, T.; Patel, D. J. *Nature* **2008**, *456*, 209–213.

(52) Teplova, M.; Wallace, S. T.; Minasov, G.; Tereshko, V.; Symons, A.; Cook, P. D.; Manoharan, M.; Egli, M. *Proc. Natl. Acad. Sci. U.S.A.* **1999**, *96*, 14240–14245.

(53) Frisch, M. J.et al. *Gaussian 03*, Revisions C.02 E. 01; Gaussian, Inc.: Wallingford, CT, 2004.

(54) Case, D. A. *AMBER 10*; University of California: San Francisco, 2008.

(55) Popenda, M.; Biala, E.; Milecki, J.; Adamiak, R. W. *Nucleic Acids Res.* **1997**, *25*, 4589–4598.

(56) Cheatham, T. E. I.; Kollman, P. A. *J. Am. Chem. Soc.* **1997**, *119*, 4805–4825.

(57) Egli, M.; Pallan, P. S. *Annu. Rev. Biophys. Biomol. Struct.* **2007**, *36*, 281–305.

(58) Harvey, S. C.; Prabhakaran, M. *J. Am. Chem. Soc.* **1986**, *108*, 6128–6136.

(59) Aurup, H.; Tuschl, T.; Benseler, F.; Ludwig, J.; Eckstein, F. *Nucleic Acids Res.* **1994**, *22*, 20–24.

(60) Hendrix, C.; Devreese, B.; Rozenski, J.; van Aerschot, A.; De Bruyn, A.; van Beeumen, J.; Herdewijn, P. *Nucleic Acids Res.* **1995**, *23*, 51–57.

(61) Manoharan, M. *Biochim. Biophys. Acta* **1999**, *1489*, 117–130.

(62) Fraser, A.; Wheeler, P.; Cook, P. D.; Sanghvi, Y. S. *J. Heterocycl. Chem.* **1993**, *30*, 1277–1287.

(63) Schmit, C.; Bevierre, M.-O.; De Mesmaeker, A.; Altmann, K.-H. *Bioorg. Med. Chem. Lett.* **1994**, *4*, 1969−1974.

(64) Barbe, S.; Le Bret, M. *J. Comput. Chem.* **2008**, *29*, 1353−1363.

(65) Venkateswarlu, D.; Lind, K. E.; Mohan, V.; Manoharan, M.; Ferguson, D. M. *Nucleic Acids Res.* **1999**, *27*, 2189−2195.

(66) Gherghe, C. M.; Krahn, J. M.; Weeks, K. M. *J. Am. Chem. Soc.* **2005**, *127*, 13622−13268.

(67) Pallan, P. S.; Prakash, T. P.; Li, F.; Eoff, R. L.; Manoharan, M.; Egli, M. *Chem. Commun.* **2009**, 2017−2019.

(68) Vicens, Q.; Gooding, A. R.; Laederach, A.; Cech, T. R. *RNA* **2007**, *13*, 536−548.

(69) Madhumalar, A.; Bansal, M. *J. Biomol. Struct. Dyn.* **2005**, *23*, 13−27.

(70) Egli, M.; Portmann, S.; Usman, N. *Biochemistry* **1996**, *35*, 8489−8494.

(71) Auffinger, P.; Westhof, E. *J. Mol. Biol.* **1997**, *274*, 54−63.

(72) Auffinger, P.; Westhof, E. *Angew. Chem., Int. Ed.* **2001**, *40*, 4648−4650.

(73) Gorin, A. A.; Zhurkin, V. B.; Olson, W. K. *J. Mol. Biol.* **1995**, *247*, 34−48.

(74) Saenger, W. *Principles of Nucleic Acid Structure*; Springer: New York, 1984.

(75) Noy, A.; Pérez, A.; Lankas, F.; Luque, F. J.; Orozco, M. *J. Mol. Biol.* **2004**, *343*, 627−638.

(76) Sponer, J.; Leszczynski, J.; Hobza, P. *Biopolymers* **2001**, *61*, 3−31.

(77) Butora, G.; Kenski, D. M.; Cooper, A. J.; Fu, W.; Qi, N.; Li, J. J.; Flanagan, W. M.; Davies, I. W. *J. Am. Chem. Soc.* **2011**, *133*, 16766−16769.

(78) Peacock, H.; Fucini, R. V.; Jaylath, P.; Ibarra, J. M.; Haringsma, H. J.; Flanagan, W. M.; Willingham, A.; Beal, P. A. *J. Am. Chem. Soc.* **2011**, *133*, 9200−9203.

(79) Yamada, T.; Peng, C. G.; Matsuda, S.; Addepalli, H.; Jayaprakash, K. N.; Alam, M. R.; Mills, K.; Maier, M. A.; Charisse, K.; Sekine, M.; Manoharan, M.; Rajeev, K. G. *J. Org. Chem.* **2011**, *76*, 1198−1211.

(80) Aigner, M.; Hartl, M.; Fauster, K.; Steger, J.; Bister, K.; Micura, R. *ChemBioChem* **2011**, *12*, 47−51.

(81) Aduri, R.; Psciuk, B. T.; Saro, P.; Taniga, H.; Schlegel, H. B.; SantaLucia, J. *J. Chem. Theory Comput.* **2007**, *3*, 1464−1475.

(82) Fox, T.; Kollman, P. A. *J. Phys. Chem. B* **1998**, *102*, 8070−8079.

(83) Ryckaert, J. P.; Ciccotti, G.; Berendsen, H. J. C. *J. Comput. Phys.* **1977**, *23*, 327−341.

(84) Darden, T.; York, D.; Pedersen, L. *J. Chem. Phys.* **1993**, *98*, 10089−10092.

(85) Lu, X. J.; Olson, W. K. *Nucleic Acids Res.* **2003**, *31*, 5108−5121.

(86) Humphrey, W.; Dalke, A.; Schulten, K. *J. Mol. Graphics* **1996**, *14*, 33−38.

(87) Lankas, F. *Biopolymers* **2004**, *73*, 327−339.

(88) Zacharias, M.; Sklenar, H. *Biophys. J.* **2000**, *78*, 2528−2542.

(89) Yang, L.; Tan, C. H.; Hsieh, M. J.; Wang, J.; Duan, Y.; Cieplak, P.; Caldwell, J.; Kollman, P. A.; Luo, R. *J. Phys. Chem. B* **2006**, *110*, 13166−13176.

(90) Boys, S. F.; Bernardi, F. *Mol. Phys.* **1970**, *19*, 553−566.